Figure 11. Rde voltammograms for the reduction of DPA in a 1.0 mM DPA–0.1 M acetonitrile solution for ω = 132 sec^{-1}. Curves a, b, and c represent repeated cathodic scans with curve a taken following oxidation of DPA at disk electrode.

at a given disk current was somewhat higher when DPA·$^+$ was generated at the disk; this is opposite to what is observed in DMF solutions. A voltammetric investigation of the reduction of DPA at the rotating-disk electrode (Figure 11) showed that these effects were

caused by an electrode surface effect during reduction. The voltammograms shown in Figure 11 were all recorded at a rotation rate corresponding to ω = 132 sec^{-1}; the alphabetization is in chronological order. Curve a was preceded by DPA oxidation at the electrode; its observed displacement in the negative direction could be the result of some surface phenomenon that is eliminated only at negative potentials. The effect shown by curve a and its cause are not critical to this discussion; they are only included here as an illustration of how electrode pretreatment can influence voltammetry. More important is the behavior exhibited by curves b and c which were obtained subsequent to curve a. Here it may be observed that the limiting current actually decreases with increasing potential; this suggests some type of filming reaction occurs which limits the flux of material into the electrode. This hypothesis was further substantiated by the appearance of a visible film on the electrode following DPA electrolysis in acetonitrile.

This filming need not be caused by DPA directly to interfere with DPA reductions. It may be that acetonitrile itself, catalyzed by the presence of DPA·$^-$, polymerizes to film the electrode. Whatever the cause, however, the effect is serious enough to limit the flux of R·$^-$ coming from either electrode in the rrde-ecl experiment.

Electrogenerated Chemiluminescence. VI. Studies of the Efficiency and Mechanisms of 9,10-Diphenylanthracene, Rubrene, and Pyrene Systems at a Rotating-Ring–Disk Electrode

J. T. Maloy and Allen J. Bard*[1]

Contribution from the Department of Chemistry, The University of Texas at Austin, Austin, Texas 78712. Received January 13, 1971

Abstract: The actinometric calibration of the rotating-ring–disk electrode (rrde) system allowed the determination of the electrogenerated chemiluminescence (ecl) efficiency, Φ_{ecl}, for several systems of interest. The efficiency for 9,10-diphenylanthracene (DPA) ecl in dimethylformamide solutions was below 0.1%. Studies performed on the DPA-tetramethyl-p-phenylenediamine (TMPD) system showed that ecl occurs during reaction of DPA·$^-$ with either TMPD·$^+$ or TMPD^{2+}; the efficiency for this ecl is about an order of magnitude smaller than for DPA alone. TMPD was also shown to be an effective quencher of DPA ecl in these systems. Rrde studies of the rubrene (R) system demonstrated that Φ_{ecl} was much smaller for it than for the DPA system and that reaction of R^{2+} with R·$^-$ or R^{2-} with R·$^+$ produced light at high rotation rates. A detailed study of the pyrene (P)–TMPD system was undertaken. The Φ_{ecl} for the P–TMPD system was smaller than that for the DPA–TMPD system. A study of the relative pyrene excimer to monomer emission in both ecl and fluorescence demonstrated the existence of a direct path to excimer in ecl, consistent with the triplet–triplet annihilation mechanism. Quenching of pyrene ecl by TMPD was also investigated.

It is of considerable interest in studies of electrogenerated chemiluminescence (ecl) to determine the overall ecl efficiency, Φ_{ecl}, which represents the frac-

(1) To whom correspondence and requests for reprints should be directed.

tion of radical ion encounters which ultimately result in the emission of a photon. Studies of ecl at the rotating-ring–disk electrode (rrde) are ideally suited for such efficiency measurements, since the radical ion precursors are generated continuously under steady-state

conditions and the fraction of the disk-generated species reacting with the ring-generated species can be determined from results of digital simulations, previously reported.[2] In particular, it was shown that when the rate of the radical ion annihilation reaction is very rapid and the ring-generated species (C) is being generated at its limiting current, then very little of the disk-generated species (B) reaches the ring or escapes into the bulk of the solution, and the number of encounters of B and C can be calculated from magnitude of the disk current, i_d. Under these conditions the intensity of ecl emission, I, is given by

$$I = 0.62\Phi_{ecl}A_D C_A^0 D_A^{2/3}\nu^{-1/6}\omega^{1/2} \qquad (1)$$

where A_D is the area of the disk electrode, C_A^0 is the bulk concentration of the parent species (A), D_A is the diffusion coefficient of A, ν is the kinematic viscosity, and ω is the angular velocity of the rrde. Combination of (1) and the Levich equation for the current at the disk electrode yields the following equation for determining Φ_{ecl}.

$$\Phi_{ecl} = nFI/i_d \qquad (2)$$

Once the rrde spectrometer system is calibrated to yield I in photons per second, then Φ_{ecl} can be determined for a given system. This paper deals with the actinometric method employed in this calibration and the results for Φ_{ecl} for several different systems.

Another application of ecl studies at the rrde involves the simultaneous measurement of steady-state i_d and I as a function of disk potential, E_d, during continuous production of the appropriate reactant at the ring electrode. These experiments provide direct information about the role of any disk-generated species in the light-producing processes. Studies such as these, described for several different systems, yielded information concerning the nature of the species which produce chemiluminescence.

Experimental Section

Experimental techniques and apparatus have been described previously.[2] The 9,10-diphenylanthracene (DPA) (mp 249–253°), rubrene (R) (mp >300°), and pyrene (P) (*purissimum*) were supplied by Aldrich and used as received. The dihydrochloride of $N,N,-N',N'$-tetramethyl-p-phenylenediamine (TMPD) was supplied by Eastman Organic Chemicals. This was neutralized in aqueous solution with sodium carbonate and the amine was extracted with petroleum ether. The extract was passed through a column of activated alumina and the solvent was evaporated from that which was eluted from the column. The sample was vacuum sublimed and then stored in the dark under an inert helium atmosphere.

Potassium ferrioxalate used in the chemical actinometry experiments was synthesized in a dark room under a red photographic safelight according to the procedure given by Calvert and Pitts.[3] Stoichiometric amounts of ferric chloride and potassium oxalate were mixed in solution to precipitate the photosensitive ferrioxalate which was recrystallized three times from water. Prepared in this way, less than 0.0005% (spectrophotometrically determined) of the iron was present as Fe(II). Since potassium ferrioxalate actinometry employs the photoconversion of Fe(III) to Fe(II) as the quanta-measuring step, this residual Fe(II) can be thought of as a background measurement; this level was acceptable. The ferrioxalate was stored in a light-tight box so that it was never exposed to any visible radiation other than the safelight.

Quinine bisulfate (NF) was purchased from the City Chemical Corp. and was used as received.

(2) J. T. Maloy, K. B. Prater, and A. J. Bard, *J. Amer. Chem. Soc.*, 93, 5959 (1971).

(3) J. G. Calvert and J. N. Pitts, "Photochemistry," Wiley, New York, N. Y., 1966, Chapter 7.

The cell and rrde were the same as previously described,[2] except that in some experiments performed to study concentration effects the cell had no "basket" so it was not possible to use this cell for experiments which were conducted at high rotation rates. In addition, the rrde was somewhat closer to the bottom of the cell, so that the optical path of the chemiluminescent emission was slightly different; correspondingly higher ecl intensities were observed with it. This cell was also fitted with two additional joints at the top. One was used to introduce an additional platinum wire microelectrode into the solution; this was used exclusively for independent cyclic voltammetric determinations of concentration. (While this could have been performed at either the stationary-ring or disk electrode, it was feared that long-term filming effects during the rrde-ecl experiment might affect the result of this cyclic experiment.) The second joint permitted a high-pressure bulb solution reservoir to be attached to the cell.

This high-pressure bulb solution reservoir was designed to add solution to the cell during the course of an experiment while keeping the cell fixed in the spectrophotofluorometer. In use, it was evacuated so that solution could be drawn up into it and degassed by the freeze–pump–thaw method; no more than half the bulb volume was ever taken up with solution. After having been degassed, the solution was frozen in liquid nitrogen under 1 atm of helium; then the stopcock was closed and the solution was allowed to thaw. This, of course, resulted in a high helium pressure inside the bulb so that when the bulb was inverted the solution inside could be injected under helium pressure into the cell which had already been sealed under 1 atm of helium. This assembly was used where concentrations were varied during the course of the experiment.

The bath used in the actinometry experiments was a tapered beaker which had been equipped with a bubbler for the exclusion of oxygen from the actinometry solutions which were used. It was tapered like the rrde cell so that when the cell was immersed in the bath, 100 ml of solution would cover the cell to a depth of at least 1 cm at all points below the plane of the electrode. The bath was covered on the outside with a foil reflector. The light-tight box used in these experiments was constructed of 0.5-in. plywood and fitted with a single lid which rested on a recessed 2-in. flange which completely framed the opening. The lid was held in place with two thumbscrews which pressed the lid against a rubber gasket which covered the flange. All interior joints were calked and the box was painted inside and out with flat black paint to absorb any stray emission. The box was also equipped with two electrical connectors and a tightly coiled length of copper tubing which served as a helium entry port; these fittings were similarly calked and painted. The photosensitive compound used in chemical actinometry was stored in this box for several months with no deleterious effects; hence, there was no reason to question the effectiveness of the box in excluding light.

Results and Discussion

Actinometric Experiments. In order to measure Φ_{ecl}, a method had to be devised to determine the absolute intensity of the chemiluminescent emission generated at the rrde. Since the cell geometry was invariant, it was quite easy to obtain reproducible measurements of relative intensity in arbitrary photomultiplier meter readings. The problem, then, was one of converting meter units (divisions) to units of absolute intensity (einsteins per second). The geometry of the optical system was kept as constant as possible so that no additional geometric corrections were required; 1-mm slits were used in all calibration and experimentation.

Since the cell had somewhat unusual geometry, it was difficult to estimate what fraction of the total ecl emission was actually being detected by the photomultiplier or to correlate an intensity observed in rrde ecl with an intensity observed from a fluorescence measurement. Therefore, no attempt was made to calibrate the photomultiplier with fluorescence techniques. Rather, it was thought best to determine the absolute intensity of ecl emission by immersing the cell in an
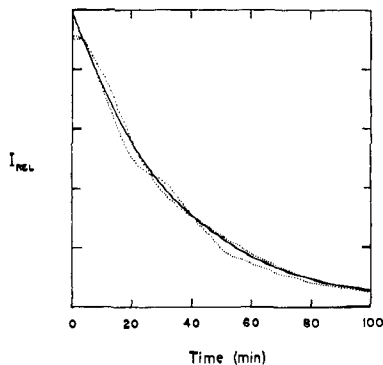
Figure 1. Long time decay of DPA ecl at rrde. DPA·+ generated at the disk at 30 μA, DPA·⁻ produced at ring at −1.93 V. vs. sce; 2 mM DPA in 0.1 M TBAP–DMF.

actinometeric bath while constant chemiluminescence was being generated for a known time interval. The average absolute intensity determined in this way could then be correlated with the wavelength-integrated meter reading obtained from the same chemiluminescence. Potassium ferrioxalate was the photosensitive compound used in the actinometric bath. Chemical actinometry using this compound was developed by Parker and Hatchard,[4] and its use has become so common that it is reported as "the best solution-phase actinometer" by Calvert and Pitts.[3] The bath was designed so that when the cell was immersed in 100 ml of 0.15 M $K_3Fe(C_2O_4)_3$ solution, its bottom was completely covered with solution to a depth of 1 cm. At the wavelengths of DPA ecl, this depth is sufficient to absorb more than 95% of the light passing through the cell That light which is absorbed converts Fe(III) to Fe(II) in acid solution with a quantum efficiency of ∼1.2. The Fe(II) produced is determined spectrometrically using 1,10-phenanthroline in a pH 3.5 buffer at 510 nm. All operations were carried out in darkroom conditions under a red photographic safelight. Since the intensity of ecl emission was quite low, 10-cm cells were used in the spectrophotometric determination of Fe(II) complex. This low light level also demanded the careful exclusion of oxygen from all solutions so that the Fe(II) which formed would not be oxidized back to Fe(III); hence, all solutions were degassed with nitrogen bubbling prior to use and the actinometric bath itself was bubbled constantly with helium during its use. The calibration curve for Fe(II) concentrations of 0.5 to 10 μM yielded a molar extinction coefficient of 1.10 ± 0.01 × 10⁴ M^{-1} cm⁻¹ for the Fe(II)–1,10-phenanthroline complex, in excellent agreement with the value found for higher concentrations of Fe(II).[3] This agreement demonstrates that air oxidation of Fe(II) does not seem to be a serious source of error even at these low concentrations. The calibration can be used to predict the minimum number of quanta which can be detected with this technique. If the minimum readable spectrophotometric absorbance is taken to be ∼0.01, the minimum detectable [Fe(II)] is ∼10⁻⁷ M; with the final actinometric solution volume of 140 ml used here, this means that ∼10⁻⁸ mol of quanta are detectable.

Initially, it was hoped to use the rrde ecl from DPA as the source of light for the calibration experiment,

and several calibration experiments were attempted by generating DPA·+ at the disk at a constant current of ∼30 μA while maintaining the ring at a potential sufficient to produce DPA·⁻. Since a disk current of ∼30 μA produced DPA·+ at the rate of ∼10⁻⁶ mol/hr, a detectable number of quanta would have been generated in 1 hr even if the overall ecl efficiency was as low as 1%. No detectable conversion of Fe(III) to Fe(II) was found, however. Intensity–time studies performed on the DPA system demonstrated why ecl from DPA could not be used as a light source for calibration. The results of these studies are shown in Figure 1, where the dotted lines show the intensity of ecl emission obtained in separate experiments as a function of time; in each experiment, 2 mM DPA solutions were subjected to a constant anodic current (about 30 μA) applied at the disk while a fixed potential (−1.93 V vs. sce) was maintained at the ring and the electrode was rotated at a constant rate. The solid line is an exponential curve with a "lifetime" of about 33 min. Thus, the ecl obtained in the constant-current experiment described above is an exponentially decaying function of time. Since the decay is exponential with a lifetime of 33 min, approximately 95% of the maximum number of quanta which can be emitted have been emitted after 100 min; therefore, there was little to be gained by exposing the actinometry solution for longer periods of time. This indicated that some other light source had to be devised for actinometric calibrations.

Figure 1 also illustrates the good reproducibility of results. The long-term depletion of electroactive species (DPA) was clearly not the cause for the decay of ecl. Since the total ring and disk current was less than 300 μA, a maximum of ∼10⁻⁵ mol of DPA could be removed from the solution in 1 hr of electrolysis. With a solution volume of 50 ml, this represents a change in bulk concentration of ∼0.2 mM, or a depletion of about 10% of the DPA initially present; during that same time interval, the ecl intensity had decreased by 80% of the initial intensity.

The experiment described above was repeated, this time with regular interruptions of electrolysis so that the solution could be scanned with cyclic voltammetry to detect the presence of any new electroactive species which might either react with the radical ions of DPA or quench the emission from its excited states. Even though an independent electrode was used exclusively for these cyclic scans, no new electroactive species were ever detected; in fact, the extent of DPA depletion by electrolysis at the rrde was indeterminable by cyclic voltammetry. One fact was determinable, however: the long-term decay of ecl emission was accompanied by a similar decrease in the lifetime of the DPA radical cation. At the conclusion of an hour of electrolysis, an attempt was made to measure the lifetime of DPA·+ with the rrde techniques which had previously proved successful;[2] its decay was too rapid to be measured at any attainable rotation rate.

Since the ring current exceeded the disk current in the experiments described above, the net effect in the bulk of the solution was a gradual build-up of the ring-generated species or a product resulting from it. If the observed decrease in cation lifetime was responsible for the decrease in ecl intensity, it is doubtful that it can be attributed to the direct reaction of DPA·+ with
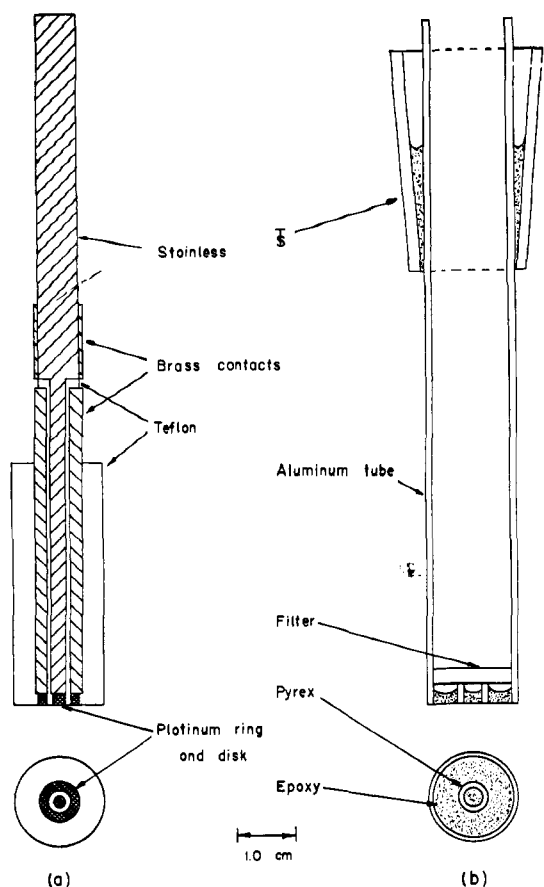
(4) C. A. Parker, Proc. Roy. Soc., Ser. A, 220, 104 (1953); Trans. Faraday Soc., 50, 1213 (1954); C. G. Hatchard and C. A. Parker, Proc. Roy. Soc., Ser. A, 235, 518 (1956).

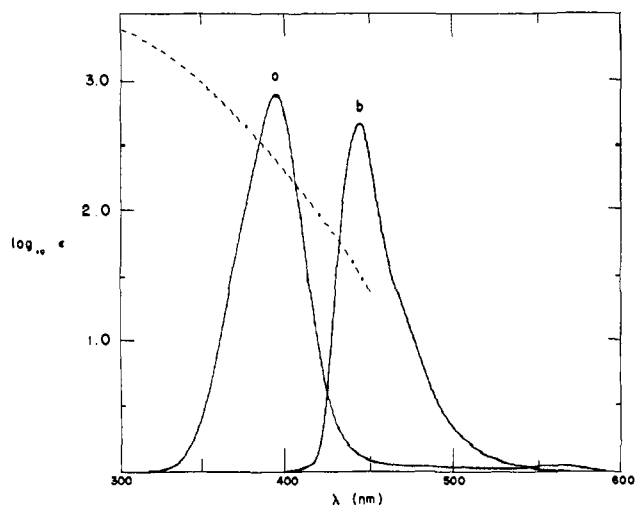Figure 2. (a) Scale drawing of rrde; (b) the rrde surrogate, used in actinometric calibration studies.

Figure 3. (a) Emission spectrum of rrde surrogate; (b) ecl emission spectrum of DPA. Dashed line shows absorption spectrum of potassium ferrioxalate actinometry solution.

residual DPA$\cdot^-$ in solution; after all, this was the process responsible for the initial high-intenisty ecl. Rather, a direct reaction with some product of DPA$\cdot^-$ must be suggested as a means of lowering the apparent lifetime of DPA$\cdot^+$, and it is worth noting that DPA$\cdot^-$ is a base. Hence, the long-term build-up of DPA$\cdot^-$ could serve to lower the acidity of the solution thereby rendering DPA$\cdot^+$ subject to basic attack.

Whatever the cause of these long-term effects, however, two important experimental techniques resulted from their observation. Care was always taken to work with fresh solutions using the minimum electrolysis time necessary to obtain meaningful data. When possible, the processes occurring at the ring and disk were alternated so that there would be no long-term buildup of either ionic species.

The Rrde Surrogate. Since it was impossible to use the ecl from DPA as light source for actinometric calibrations, a surrogate rrde was constructed to produce a constant light of essentially the same geometry and wavelength as that observed from ecl. This device, shown in Figure 2b, was designed to have the same geometry as the rrde (Figure 2a) and care was taken that both it and the rrde extended the same depth into the cell. Not shown in this figure is the incandescent bulb which was suspended inside the aluminum tube as a light source. The actual diameter of the Pyrex tube at the base of the surrogate was 5 mm; this was selected to approximate the size of the ring of light observed in rrde ecl. When the incandescent bulb had become aged and was operated at a low level of constant current,

it was found that the integrated intensity of the emission was invariant within 10% over a 24-hr period; hence, the filtered bulb, operated at constant current with a Princeton Applied Research Model 170 electrochemistry system, proved to be a reliable constant intensity source.

A spectrum of the filtered emission resulting from the rrde surrogate immersed in cyclohexane within the ecl cell is shown as curve a in Figure 3. In the same figure, the initial DPA ecl spectrum from the experiments at the rrde is shown as curve b; both curves were recorded under the same set of optical conditions, so the integrated intensity of each source was nearly the same. The dotted line in the same figure shows the absorption spectrum of the potassium ferrioxalate actinometry solution as reported by Parker.[4] Note that the filter which was selected for the rrde surrogate removed all of the low-energy portion of the incandescent continuum; that portion of the spectrum which remained was easily absorbed by the actinometer, perhaps somewhat more readily than DPA emission. Still, the spectral regions of the two bands were considered close enough so that no detector sensitivity correction was considered necessary to compare the integrated intensity of the two bands.[5] Since the emission from the rrde surrogate was of the same magnitude as the intensity of DPA ecl, it was found that long exposure times were still required to convert a detectable amount of Fe(III) to Fe(II) in the chemical actinometer; in the final calibration experiment performed, an exposure time of 22 hr was employed.

In this experiment, the actinometry solution was prepared just as in the previous experiments with DPA, but after the initial spectra had been recorded, the entire actinometry apparatus was set up in a light-tight box. This box was equipped with a helium port, so that the solution could be continuously bubbled with helium and fitted with light-proof electrical contacts for the bulb. Constant current of the same magnitude used to obtain spectra was supplied to the bulb through a relay circuit which was designed to mark the termination of the experiment in the event of filament burn out.
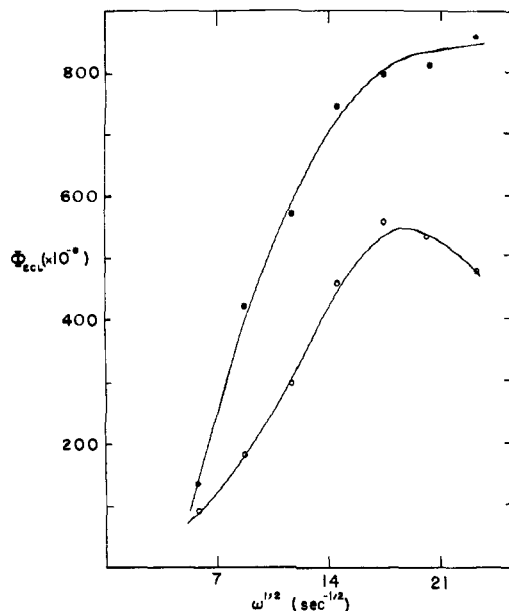
(5) R. F. Chen, *Anal. Biochem.*, 20, 339 (1967).

Figure 4. Efficiency of DPA ecl at various rotation rates: ●, disk generation of DPA·⁻; ○, disk generation of DPA⁺.

At the conclusion of the experiment, the box was opened under darkroom conditions and the actinometry solution was treated as before to determine the number of quanta emitted. The spectrum was again recorded at the same current level so that the integrated spectrum both before and after actinometry was known. In this experiment, 7×10^{-8} mol of Fe(II) was produced in 8×10^4 sec. This corresponded to an average absolute intensity of 7×10^{-13} einstein/sec. The mean integrated intensity of the spectrum recorded for this emission was 3.2×10^3 division nm. Hence, the conversion factor determined in this manner for converting an integrated spectrum to units of absolute intensity was $(2.3 \pm 0.2) \times 10^{-16}$ (einstein sec⁻¹)/(division nm), where the range indicated is the average deviation between two measurements. To use this calibration data with other compounds having emission in different regions of the spectrum, experiments were performed to determine the sensitivity factor for the photomultiplier (RCA 1P21) and emission grating system of the Aminco-Bowman instrument used. The sensitivity factor, $S(\lambda)$, was found by comparison of the recorded fluorescence spectrum of quinine bisulfate with that reported in the literature.[6] The sensitivity factor was determined using a 10^{-4} M quinine bisulfate–0.25 M H_2SO_4 solution with an excitation wavelength of 333 nm. Since the sensitivity was found to be uniform in the region of 350–500 nm, no corrections were needed between the calibration and DPA and pyrene ecl. However, a suitable correction factor was applied in studies of rubrene ecl.

Ecl Efficiency for DPA. Using the calibration factor, the ecl intensities, I, previously determined[2] can be used, via (2), to obtain Φ_{ecl}. Intensity at the wavelength of maximum DPA emission was used to calculate total integrated intensity by integration of the ecl spectra obtained for DPA (Figure 3) and computation of the appropriate area–height ratio (47 nm). This could then be used to calculate Φ_{ecl} resulting when either radical

ion of DPA was generated at the disk as a function of rotation rate. The results of this calculation appear in Figure 4, where the open circles represent data for DPA·⁺ and the filled circles DPA·⁻ generated at the disk. These data indicate not only that Φ_{ecl} generally increases with ω, but also that in DMF the generation of DPA·⁻ at the disk is always more efficient at producing light than the disk generation of DPA·⁺. They also indicate that ecl is not a very efficient means of producing light; the maximum efficiency observed with DPA is less than 0.1%. This, however, is the highest efficiency observed for any ecl process reported here.

The DPA–TMPD System. It is of interest to compare the Φ_{ecl} of a system involving only DPA·⁻ and DPA·⁺ annihilation, an "energy-sufficient" system (i.e., a system where the energy of the emitted light is less than the enthalpy of the redox reaction for a single pair of reacting species producing ground-state products) to that involving DPA·⁻ and TMPD·⁺, an "energy-deficient" system. The intensity of ecl emission from the DPA·⁻–TMPD·⁺ system shows a magnetic field dependence,[7] which is consistent with a mechanism involving initial production of triplet DPA, followed by triplet–triplet annihilation to yield excited DPA singlet. There is some question of applying the digital simulation treatment for the energy-sufficient case to mixed systems, such as DPA–TMPD. The digital simulation described previously[2] involved only three species, the parent hydrocarbon present initially and its radical ions; an exact treatment of the problem specified above would involve four species: DPA, DPA·⁻, TMPD, and TMPD·⁺, two of which are present initially. This problem presents some interesting nuances, not the least of which is the fact that large quantities of two species will always be swept from the disk region to the ring region. That is, if DPA·⁻ is generated at the disk, TMPD will be electroinactive at the disk potential, and therefore it will be present in bulk concentration in that volume of solution which is directly below the disk. Hence, the disk region will be a source of not only DPA·⁻ but also TMPD for the ring, and the rapid reaction of disk-generated DPA·⁻ and ring-generated TMPD·⁺ is likely to occur in a solution region where the concentration of TMPD is high. Similarly, the reaction of disk-generated TMPD is likely to occur in a region where the DPA concentration is high. Nevertheless, (2) probably has limited validity if the chemical reactions preceding chemiluminescence are rapid and kinetically uncomplicated. This is because the flux of a ring-generated radical ion cannot be decreased by ceasing the generation of the oppositely charged radical at the disk; this only makes more parent hydrocarbon available at the ring. Thus, the impenetrability of the ring-generated species is not lowered in the mixed-system experiment, and the torus of ring species will be just as effective in blocking the escape of any species generated at the disk. However, with the added degree of freedom granted by the mixed system, one could certainly increase the concentration of the disk-active species so that the flux from the disk could exceed the blocking capabilities of the ring species. This critical flux from the disk that will ultimately penetrate the torus even in the limit of

(6) (a) H. C. Borresen, *Acta Chem. Scand.*, 19, 2089 (1965); (b) E. Lippert, W. Nagele, L. Seibold-Blankenstein, U. Staiger, and W. Voss, *Z. Anal. Chem.*, 170, 1 (1959).

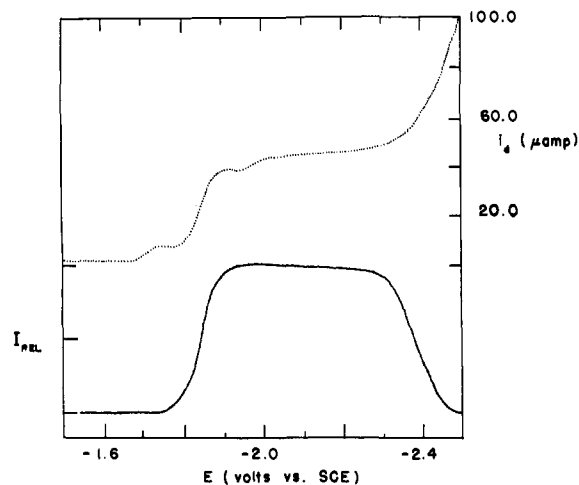(7) L. R. Faulkner and A. J. Bard, *J. Amer. Chem. Soc.*, 91, 209 (1969).

Figure 5. Steady-state current ($\cdots$) and ecl intensity (——) for the DPA–TMPD system. The solution contained 1.0 mM DPA, 1.0 mM TMPD, and 0.1 M TBAP in DMF. Ring electrode was maintained at about $+0.35$ V $vs.$ sce and disk potential was scanned from 0 to -2.5 V. $\omega = 132\,\text{sec}^{-1}$.
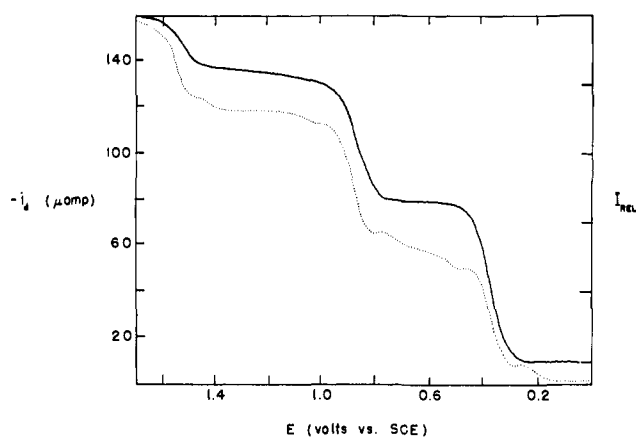

Figure 6. Steady-state current ($\cdots$) and ecl intensity (——) for DPA–TMPD system. Ring was maintained at about -2.1 V $vs.$ sce and disk potential was scanned from 0 to $+1.6$ V. Other conditions as in Figure 5.

Figure 7. Ecl intensity–current behavior of the DPA–TMPD system.

rapid reaction has not been determined. This would require a series of simulations for the mixed system problem. What is certain, though, is that the critical flux is greater than the absolute magnitude of the Levich current that would be observed at the disk if the disk were set at the potential of the ring.

The results of potential scan experiments on the mixed DPA–TMPD system are shown in Figures 5 and 6. The technique used to obtain the simultaneous recording of disk current and relative ecl intensity as a function of disk potential has been discussed previously.[2] Each experiment was performed upon a DMF solution 1.0 mM in DPA, 1.0 mM in TMPD, and 0.1 M in TBAP; the rotation rate was 132 sec^{-1} in each case. The disk current is shown as a dotted line and the relative intensity of ecl as a solid line. (The somewhat erratic current behavior, involving both prewave and postwave fluctuations, was an instrumental artifact in this experiment alone.) In Figure 5 the ring was maintained at about $+0.35$ V $vs.$ sce so that TMPD$\cdot^+$ was generated there to react with DPA$\cdot^-$ formed at the disk. The results obtained here are quite similar to those obtained when DPA$\cdot^+$ was generated at the ring; ecl is only pro-
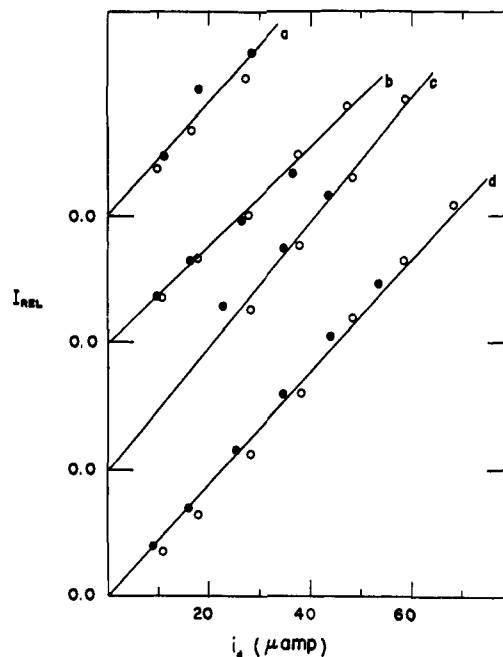
duced throughout the disk generation of the radical anion. As before,[2] either DPA$\cdot^-$ is essential to the ecl process or DPA^{2-} or a product from reduction of TBAP–DMF is a quencher of ecl. In Figure 6 the ring was maintained at about -2.1 V $vs.$ sce so that DPA$\cdot^-$ was generated there to react with species made at the disk, while the disk was scanned through potentials that would successively generate TMPD$\cdot^+$, DMPD^{2+}, and DPA$\cdot^+$. The generation of each of these species caused a corresponding increase in both disk current and ecl intensity. Thus, it seems clear that each of these oxidants reacts with DPA$\cdot^-$ to produce chemiluminescence.

Although the current levels in Figure 6 may be too high to compare the relative efficiencies of the processes involved, this experiment indicates that the selective optical detection of electrogenerated oxidants is feasible with rrde ecl.

The Φ_{ecl} for the system was determined by maintaining the ring at a fixed potential for generation of either DPA$\cdot^-$ or TMPD$\cdot^+$ and applying different constant currents, less than the limiting disk current, to the disk. The results of this constant-current experiment performed on an equimolar DPA–TMPD system are shown in Figure 7, where the relative steady-state ecl intensity is plotted against the disk current at a fixed rotation rate. The origin has been displayed for each of the four rotation rates shown, but the ordinate scale is the same for each line. The open circles represent results obtained when the ring was potentiostated at -1.93 V $vs.$ sce; hence, these show anodic disk currents. The filled circles are results obtained for cathodic currents at the disk; the ring in these cases was set at $+0.35$ V $vs.$ sce. A background current was estimated from disk voltammograms obtained at each rotation rate, and the constant disk current shown has been corrected by this amount. Since the slope of these lines is proportional to Φ_{ecl}, in this case the efficiency is independent of which species is generated at the disk,
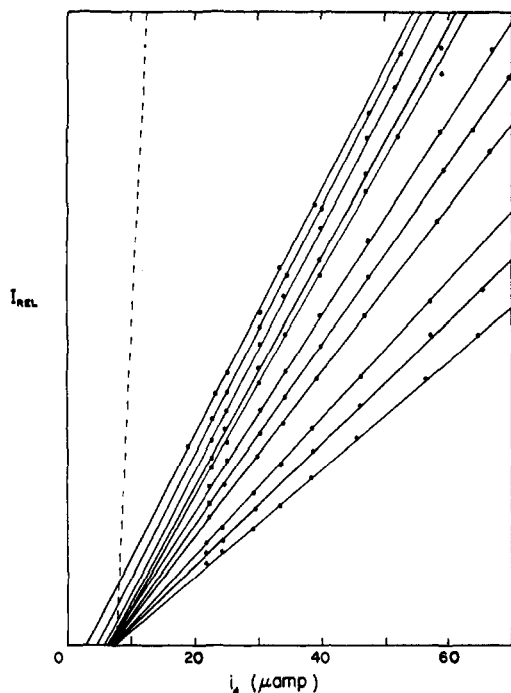
Figure 8. Ecl intensity–current behavior of the DPA–TMPD system with increasing amounts of TMPD: 1.0 mM (top line) to 7.6 mM TMPD (bottom line) concentrations of TMPD corresponding to points in Figure 9.

Figure 9. Ecl efficiency for the DPA–TMPD system as a function of TMPD concentration.

indicating that the ionic precursors to ecl are both stable in DMF. The slopes of these lines were converted to Φ_{ecl}, yielding the values given in Table I. The results

Table I. The Efficiency of DPA–TMPD Ecl

Line	ω, radians/ sec	$\Phi_{ecl} \times 10^{-6}$	Chronological order of expt
a	74	49	3
b	132	42	1
c	208	53	4
d	298	48	2

show that the efficiency is independent of the rotation rate. In fact, the slight variation in efficiency that is observed seems to be related more to the chronological ordering of the measurements than to the rotation rate. Moreover, the efficiencies observed are about 10% of those which are observed with DPA alone. This is certainly consistent with the intermediacy of easily quenched species, such as triplets, in the energy-deficient case.

Some preliminary fluorescence experiments showed that TMPD quenches the fluorescence of DPA. This is not surprising, for fluorescence quenching by aromatic amines has been known for some time and the phenomenon has been frequently investigated and interpreted.[8] The effect is usually attributed to an electron-transfer quenching process because radical ions have been observed as a product of the quenching reaction. Because this observation of TMPD quenching of DPA fluorescence raised the question of whether this quench-

(8) (a) H. Leonhardt and A. Weller, Ber. Bunsenges. Phys. Chem., 67, 791 (1963); (b) D. Rehm and A. Weller, ibid., 73, 834 (1969); (c) H. Knibbe, D. Rehm, and A. Weller, ibid., 73, 839 (1969).
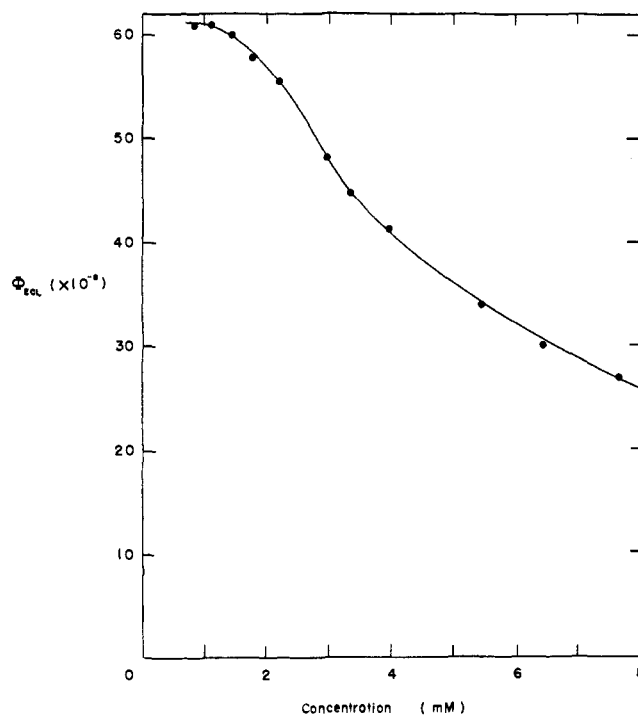
ing was responsible for the low efficiencies observed in the DPA–TMPD system, an experiment was devised to study the effect of TMPD quenching on the ecl emission of DPA. To do this, the special rrde cell fitted with the high-pressure bulb was used. The bulb was filled with a concentrated (30 mM) solution of TMPD which was to be injected into the bulk solution in small increments so that the efficiency of the ecl process could be determined at various TMPD concentrations. In order that there would be no dilution effects for the other species in solution, a DMF solution was made up initially that was 1.0 mM in DPA and 0.1 M in TBAP, and part of this solution was used to prepare the TMPD solution in the bulb. The remainder of the DPA solution was placed in the cell to initiate the experiment; hence, any solution which was added from the bulb changed only the TMPD concentration in the cell.

Efficiencies were determined by the constant-current technique with the rotation rate held constant at 132 sec^{-1}. First, the efficiency of the reaction of DPA$\cdot^+$ and DPA$\cdot^-$ was determined by generating DPA$\cdot^+$ at the disk. Then a small volume of TMPD concentrate was added to the solution from the high-pressure bulb, and the bulk concentration of TMPD was determined by cyclic voltammetry at an independent platinum electrode which had been included for this purpose. The efficiency experiment was repeated, but this time TMPD$\cdot^+$ was generated at the disk to react with DPA$\cdot^-$ generated at the ring. This process was repeated through several additions of TMPD. The result of this experiment is shown in Figure 8, where the relative ecl intensity is plotted as a function of disk current. In this experiment, no correction was made for background current so the current shown is that which was actually applied at the disk. The dashed line at the left is an extrapolation of that which was obtained for
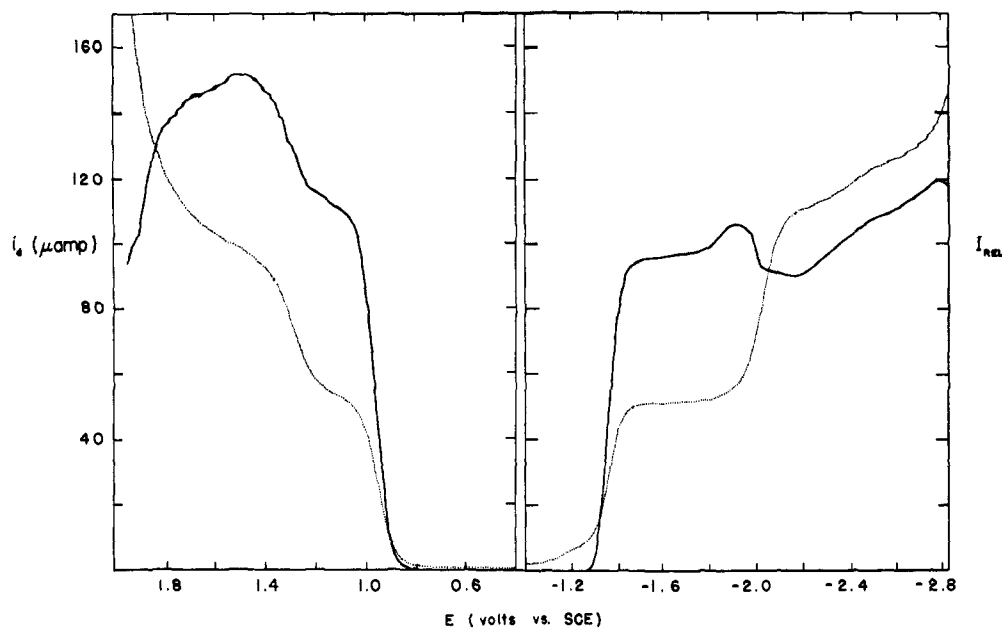
Figure 10. Steady-state current (· · ·) and ecl intensity (——) of rubrene as a function of disk potential. The solution was 1.0 mM in rubrene and the rotation rate was 298 sec^{-1}. For the scan on the left, the ring potential was about -1.4 V vs. sce; for the scan on the right, it was about $+1.1$ V.

the reaction of DPA·$^+$ and DPA·$^-$ initially; this required a photomultiplier setting ten times less sensitive than that used to obtain the remainder of the points shown. The efficiency of the reaction of the ion radicals of DPA is 620 × 10^{-6}, as determined by the slope of this dashed line. The remaining points show the variation of ecl intensity with disk current as the TMPD concentration was increased; each straight line encountered clockwise was obtained at successively higher concentrations of TMPD. Since the slope of these lines is proportional to the efficiency, it is clear that the efficiency decreases as the TMPD concentration increases. The efficiency obtained from the slopes of the lines in Figure 8 is shown as a function of TMPD concentration in Figure 9. This experiment shows the following. (1) When the bulk concentrations of TMPD and DPA are the same (1.0 mM), the efficiency shown in Figure 9 is slightly higher in this experiment that those shown in Table I. The slight differences in the geometries of the cells used in the two experiments probably account for the discrepancies between the two measurements. (2) The independent observation of a high efficiency for the radical ions of DPA reaffirms the fact that the energy-sufficient case is far more efficient. (3) TMPD is a fairly efficient quencher of DPA ecl, having an apparent half-quenching concentration of about 6.5 mM. Because the efficiency has been determined as a function of TMPD concentration, it is clear that this effect is due to TMPD and not TMPD·$^+$. Since TMPD·$^+$ is generated at constant current at the disk, the decrease in efficiency observed at constant current with increasing TMPD concentration is actually a decrease in ecl intensity per unit flux of TMPD·$^+$ and, as such, it can be attributed only to TMPD. (4) At low concentrations of TMPD, the efficiency is constant. This could imply that the concentration of TMPD in the reaction zone is too low to quench ecl emission effectively when the bulk concentrations of TMPD and DPA are equal. (5) Linear I vs. i behavior is observed even at currents of 70 µA,

which are significantly higher than the limiting current for DPA at the disk ($\sim$45 µA). This would not occur if these currents exceeded the critical flux for the ring-generated torus of DPA·$^-$ which surrounds the disk. This constitutes experimental evidence that species generated at these current levels have unit probability of reaction with DPA·$^-$ in solution.

The Rubrene System. The ecl behavior of 5,6,11,12-tetraphenylnaphthacene [or rubrene (R)] has been the subject of several studies. The cation radical, R·$^+$, is moderately stable in DMF and formation of both R^{2+} and R^{2-} is possible in DMF-TBAP solutions before background reactions occur. The enthalpy of reaction of R·$^-$ and R·$^+$ is marginal with respect to energy sufficiency, and recent experiments in our laboratories have shown that the rubrene ecl exhibits a magnetic field dependence.[9] The results of disk potential-scan experiments on a 1.0 mM solution of rubrene in DMF containing 0.1 M TBAP are shown in Figure 10. As before, the resulting disk current is shown as a dotted line while the relative ecl intensity is shown as a solid line. Again, the ring potential was held constant to generate the oppositely charged radical ion.

Since both the dianion and the dication of rubrene are stable in DMF, two distinct processes are indicated by each voltammogram. In addition, the effect of each process on the ecl process is clear, and one may calculate the efficiency of each ion from data like these. Moreover, both the oxidation and the reduction of rubrene to its radical ions are accompanied by ecl emission that is proportional to the disk current, and the limiting relative intensities observed from each process are nearly the same. The data obtained from several potential-scan experiments are shown in Figure 11. Quadrant Ia shows the limiting disk current for the reductions which produce both R·$^-$ (filled circles)

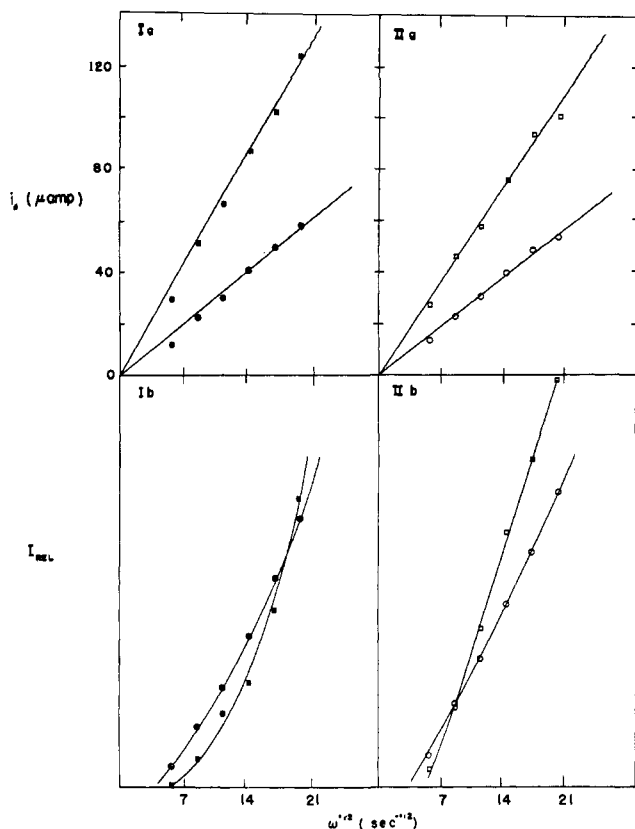(9) L. R. Faulkner, H. Tachikawa, and A. J. Bard, J. Amer. Chem. Soc., in press.

Figure 11. The limiting disk current and ecl intensity of rubrene as a function of rotation rate: filled points, data obtained during the reduction of a 1.0 mM rubrene solution at the disk; open points, oxidation; O and $\bullet$, one-electron processes; $\square$ and $\blacksquare$, two-electron processes.

Figure 12. The efficiency of rubrene ecl at various rotation rates: $\bullet$, disk generation of $R\cdot^-$; $\blacksquare$, R^{2-}; O, $R\cdot^+$; $\square$, R^{2+}.

and R^{2-} (filled squares) as a function of $\omega^{1/2}$; quadrant IIa shows the same relationships for the oxidations which produce $R\cdot^+$ (open circles) and R^{2+} (open squares). Corresponding symbols are used in the lower quadrants to show the relative limiting ecl intensity that results from each of these disk processes. Some general observations may be made concerning these results. (1) The variation of the limiting current with $\omega^{1/2}$ is linear for both the reductions and both the oxidations. These graphs show reasonable extrapolation through the origin, and within each quadrant the ratio of the slopes of these lines is 2:1, the electron ratio for the processes involved. In both quadrants, equal slopes are obtained for processes involving an equal number of electrons. The i vs. $\omega^{1/2}$ behavior is that predicted by the Levich equation. (2) At all rotation rates shown, the intensity of ecl produced by the limiting current generation of $R\cdot^+$ is almost equal to that produced by $R\cdot^-$. The relative intensity from each process increases with $\omega^{1/2}$, but not in a linear fashion at low rotation rates. This very slight curvature may be caused by a slight instability of both radical ions in DMF. (3) The generation of both R^{2+} and R^{2-} decreases the ecl intensity at low rotation rates, yet increases it at higher rotation rates. This behavior could be due to the relative instability of R^{2+} and R^{2-} at low rotation rates. Whatever the cause, the fact that the ecl curves cross in Ib and IIb indicate that some ecl-inhibiting reaction is overcome at high rotation rates so that reaction of R^{2+} with $R\cdot^-$ and of R^{2-} with $R\cdot^+$ to produce chemiluminescence can occur. (4) As was
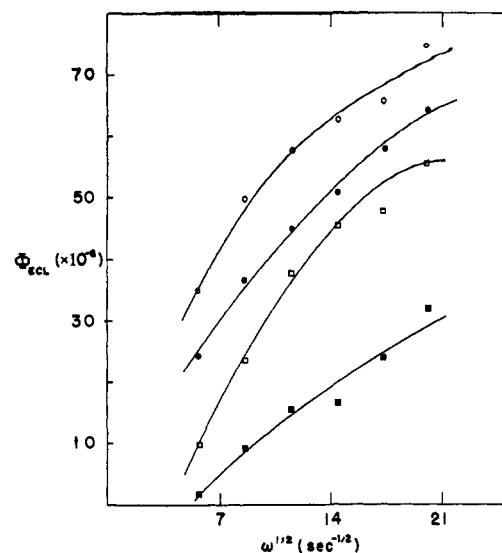
the case with DPA ecl,[2] each I vs. $\omega^{1/2}$ graph for rubrene appears to have a nonzero intercept. From the data in Figure 11 the efficiency of both $R\cdot^+$ and $R\cdot^-$ may be determined, and the efficiency of R^{2+} and R^{2-} may be estimated. This reservation must be made concerning the dication and dianion because the generation of a doubly charged species at the disk was not considered in the digital simulations. Strictly speaking, one ion of R^{2+} or R^{2-} can react with two ions of the oppositely charged radical. For example, one might propose the following scheme for the production of ecl from the disk generation of R^{2+}.

$$R^{2+} + R\cdot^- \longrightarrow R\cdot^+ + R^* \qquad (3)$$
$$R\cdot^+ + R\cdot^- \longrightarrow R + R^* \qquad (4)$$
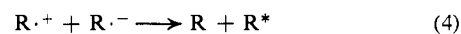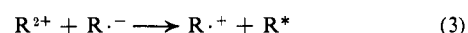
In this two-step process, each dication effectively removes two radical anions from the reaction zone so that R^{2+} is twice as effective as $R\cdot^+$ at removing the $R\cdot^-$ which surrounds the disk, and there may not be unit probability that all the R^{2+} generated at the disk will react with $R\cdot^-$ generated at the ring. However, since the actual course of the reaction is not yet known, it did not appear fruitful to simulate this case, and Φ_{ecl} for the dication and the dianion was calculated from (2) assuming that its validity requirements were not violated. Therefore, Φ_{ecl} was calculated for each disk reaction by dividing the total ecl intensity by the total faradaic current at the disk. In this manner, the efficiency of the reaction of $R\cdot^+$ and $R\cdot^-$ was determined from the generation of either species at the disk, while the efficiencies of the reactions of R^{2+} and $R\cdot^-$ or R^{2-} and $R\cdot^+$ were determined by generating only the doubly charged species at the disk. The intensity of the rubrene emission was corrected for photomultiplier sensitivity and integrated area under the rubrene spectrum, as previously described. The results of these determinations are shown in Figure 12, where the plotting symbols correspond to those given in Figure 11. Recent results by C. P. Keszthelyi in our laboratories, employing a Hamamatsu R456 phototube instead of the 1P21 phototube, suggest that the sensitivity correction did not fully account for the considerable amount of emission from rubrene at wavelengths above 600 nm. The
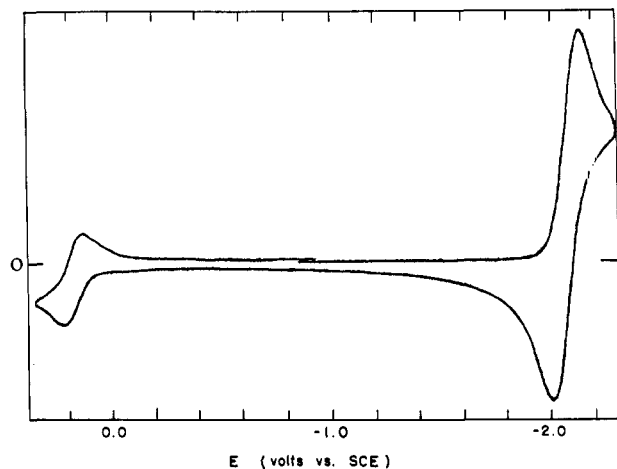
Figure 13. Cyclic voltammogram of pyrene–TMPD system at platinum electrode. Solution contained 5.0 mM pyrene and 1.0 mM TMPD in 0.1 M TBAP–DMF.

actual Φ_{ecl} for the rubrene system could then be five to ten times the values shown in Figure 12. From this figure the following observations can be made about Φ_{ecl}, for rubrene. (1) The efficiency of all processes increases with increasing ω. (2) The efficiency obtained by generating R·$^+$ at the disk is not much different from the efficiency obtained from the disk generation of R·$^-$, but it may be somewhat higher at all rotation rates. (3) On the basis of our assumptions, both R^{2+} and R^{2-} appear to be less efficient at producing ecl than either radical ion.

The Pyrene–TMPD System. Ecl of the mixed system pyrene (P)–TMPD has been reported previously.[10] This system is of particular interest in ecl studies because pyrene was one of the first compounds studied by delayed fluorescence to demonstrate the feasibility of the triplet–triplet annihilation mechanism in solution.[11] Since the reaction of pyrene and TMPD is energy deficient, the pyrene ecl which is observed from this reaction should exhibit some of the same properties as the delayed fluorescence of pyrene if the triplet–triplet annihilation hypothesis is a valid explanation of energy deficient ecl.

The cyclic voltammetry of the pyrene–TMPD system in DMF with 0.1 M TBAP supporting electrolyte is shown in Figure 13. For this particular voltammogram, the pyrene concentration was five times that of the TMPD; hence, the pyrene reduction appears at -2.14 V vs. sce at the larger of the two waves, while TMPD oxidation occurs at $+0.24$ V vs. sce. From this voltammetry it is clear that both radical ions are stable in DMF. The formation of TMPD^{2+} and P·$^+$ is not shown in Figure 13. Pyrene is oxidized very close to the anodic limits of the DMF–TBAP solvent system, and no stability is indicated electrochemically for the pyrene cation.

The fluorescence spectrum of 5.0 mM pyrene in DMF is shown as the uppermost curve in Figure 14. The two major peaks in this spectrum occur at 393 and 470 nm; these correspond to emission from the excited pyrene monomer (P*) and the excited pyrene dimer (P$_2$*), respectively. As first observed by Förster and

(10) J. T. Maloy, K. B. Prater, and A. J. Bard, *J. Phys. Chem.*, **72**, 4348 (1968).

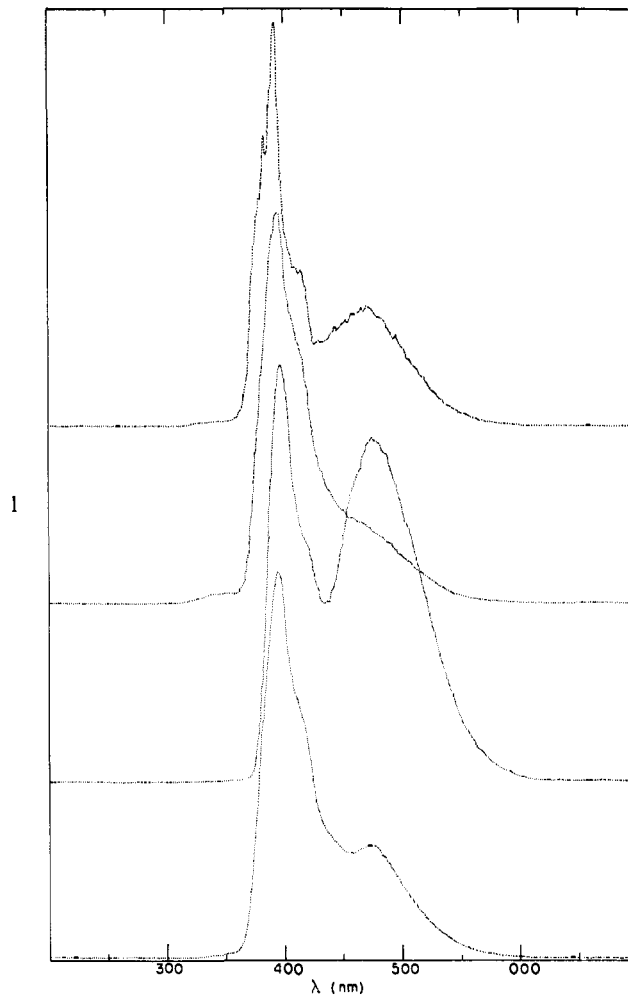(11) C. A. Parker, *Advan. Photochem.*, **2**, 305 (1964).

Figure 14. Spectroscopic studies of the pyrene–TMPD system. The upper fluorescence spectrum is of 5.0 mM pyrene in DMF. The lower three spectra were obtained in the additional presence of 1.0 mM TMPD and 0.1 M TBAP and show preelectrolysis fluorescence, ecl, and postelectrolysis fluorescence, respectively.

Kasper,[12] the relative excited dimer (excimer) emission increases with increasing pyrene concentration; hence, at low concentration only the (better resolved) pyrene monomer spectrum appears. The second curve in this figure shows the preelectrolysis fluorescence spectrum of a DMF–TBAP solution of 5.0 mM pyrene and 1.0 mM TMPD. Note that, relative to the monomer emission, the excimer emission has been diminished by the presence of TMPD. The third curve shows the ecl spectrum that is obtained from the same solution. In ecl, the relative excimer emission is much larger than that observed in fluorescence. Finally, the lowest curve shows the postelectrolysis fluorescence spectrum of the same solution. No new fluorescent bands appear, but the long-term depletion of TMPD is probably responsible for the slight increase in relative excimer emission following electrolysis.

Both potential-scan and constant-current experiments were performed on the pyrene–TMPD system. The potential-scan experiments were used to determine the I vs. E characteristics for the system; the efficiency of the reaction was determined by constant-current techniques. The results of the potential-scan experi-

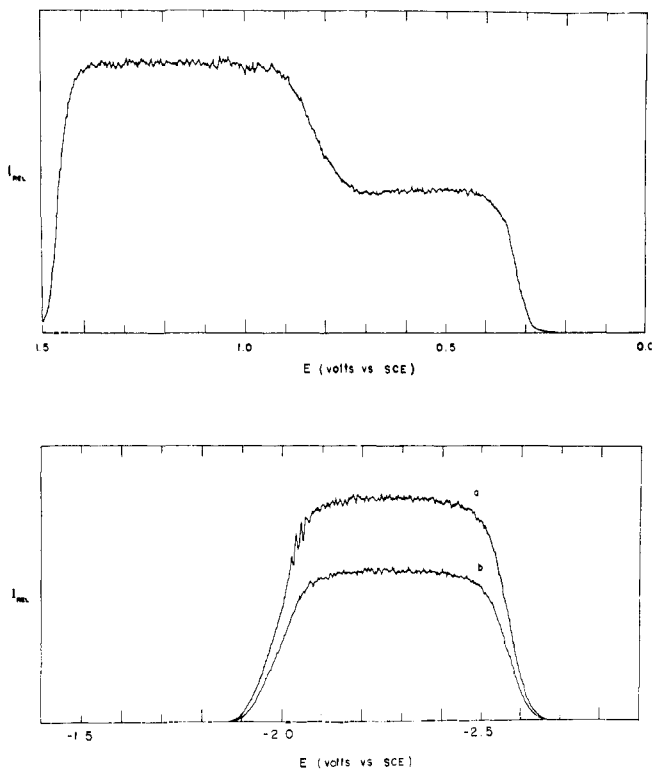(12) Th. Förster and K. Kasper, *Z. Elektrochem.*, **59**, 977 (1955).

Figure 15. Steady-state ecl intensity–disk potential behavior for pyrene–TMPD system. Upper curve, P·⁻ generated at ring (emission at 393 nm); lower curve, TMPD⁺ generated at ring (emission at (a) 393 and (b) 470 nm).

Figure 16. Ecl intensity–current behavior of pyrene–TMPD system at different rotation rates. Data as in Table II.

ments are shown in Figure 15. The ecl behavior is well defined and similar to that obtained previously. The upper figure shows the ecl behavior observed at 393 nm when P·⁻ was generated at the ring while the disk was scanned through positive potentials. The oxidation of TMPD to form both TMPD·⁺ and TMPD²⁺ is seen to produce pyrene chemiluminescence, and each disk generated oxidant is responsible for a distinguishable increase in steady ecl intensity. Unlike the DPA–TMPD system, however, the pyrene–TMPD system exhibits no increase in ecl intensity at high positive potentials. In fact, as shown in Figure 15, the ecl intensity actually decreases at high potentials. Since the generation of TMPD²⁺ continues at these potentials, this indicates that a species generated at the disk quenches pyrene ecl. Because the pyrene cation is formed at these potentials, it is very possible that it is the quenching agent, but one cannot rule out solvent decomposition products in this regard since the solvent is also oxidized at these potentials. This latter process, however, was not deleterious to the ecl emission from DPA. The lower scan in Figure 15 shows the I vs. E behavior when TMPD·⁺ was generated at the ring while the disk was scanned through negative potentials. Curve a was observed at 393 nm and b at 470 nm to determine if the relative excimer emission exhibited any potential dependence; clearly, it did not. In addition, these curves illustrate that pyrene ecl, like that of DPA, requires the specific generation of the anion radical.

The efficiency of the reaction of P·⁻ and TMPD·⁺ was determined by constant-current techniques applied to a DMF solution that was 5.0 mM in pyrene and 1.0 mM in TMPD. The results obtained in this manner
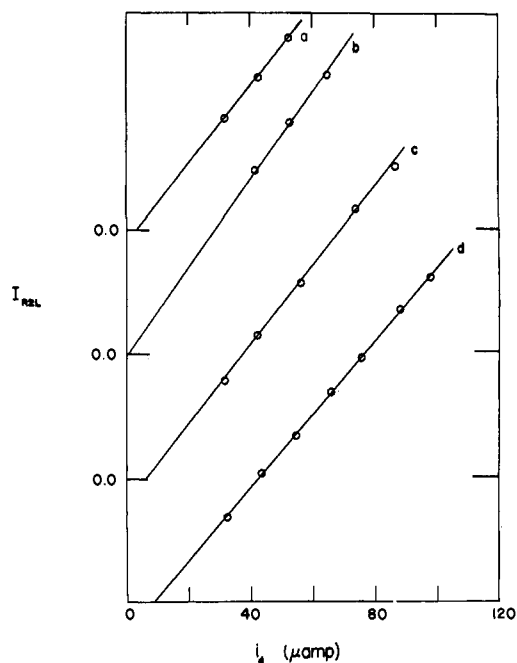
are somewhat different from those obtained for the DPA–TMPD system in that the efficiencies obtained by generating P·⁻ at the disk were much less than those obtained by generating TMPD·⁺ at the disk. Therefore, only the results of generating constant oxidative disk currents at various rotation rates are shown in Figure 16. These currents are uncorrected for background so that they represent that which was actually applied at the disk. As in Figure 7, the origin has been displaced for each rotation rate shown, but the ordinate scale is constant throughout. Thus, the differential efficiency is represented by the slope of each line.

Since the ecl spectrum of pyrene is more complicated than that of DPA, the ecl intensity was found by obtaining a complete spectrum at each constant disk current and integrating it by cut-and-weigh techniques. Because pyrene emission is in the region of linear photomultiplier response, no sensitivity corrections were required. The efficiencies obtained by this method for the data in Figure 16 are given in Table II. For com-

Table II. The Ecl Efficiency of the Pyrene–TMPD System

Line (Figure 16)	ω, radians/ sec	Φ_{ecl} × 10⁶	Chronological order	Disk-generated species
a	132	6.9	2	TMPD·⁺
b	208	7.8	1	TMPD·⁺
c	298	7.1	3	TMPD·⁺
d	530	6.6	4	TMPD·⁺
	208	1.3		P·⁻

parison purposes, an efficiency obtained in a similar manner by generating P·⁻ at the disk is also included in this table.

On the basis of the results obtained from these constant-current experiments, the following observations can be made. (1) Energy-deficient pyrene ecl increases

linearly with anodic disk current, indicating that the reactions producing ecl are rapid. (2) There is very little rotation-rate dependence on the efficiency of the process. (3) The efficiency of this process is lower than that observed for the DPA–TMPD system. Although this effect could be explained by a variety of causes, it could be the result of highly efficient quenching of pyrene ecl by TMPD. (4) The efficiency observed by generating $P\cdot^-$ at the disk is much lower than that observed when $TMPD\cdot^+$ is generated at the disk. Since the flux of $P\cdot^-$ across the ring is necessarily accompanied by a larger flux of TMPD, this effect, too, could be the result of TMPD quenching.

General Mechanism of Excimer Emission. The relative excimer emission (the ratio of the integrated excimer emission to the integrated monomer emission) from pyrene is of interest because it depends not only upon the rate constants for the various processes involved but also upon the relative rate of formation of each excited species. In prompt fluorescence, all the excimer emission observed results from the reaction of a ground-state molecule (A) with one in the excited state

$$A + A^* \longrightarrow A_2^* \qquad (5)$$

so that there is no direct way to form A_2^* without first forming A^*. In delayed fluorescence, the reaction proceeds at a slower rate via triplet intermediates so that the direct formation of the excimer, via (6), is possible.

$$^3A + ^3A \longrightarrow A_2^* \qquad (6)$$

This additional mode of excimer formation results in the observation of higher relative excimer emission in delayed fluorescence at a given concentration of A.

The steady-state treatment of the mechanism proposed for this process has been given by Parker and coworkers[13,14] and by Birks.[15] Both authors consider the scheme

$$(7)$$
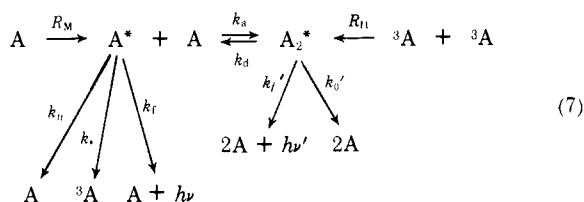
where k_f and k_f' are the rate constants for the radiative transitions of the monomer and the excimer, k_0 and k_0' are the respective rate constants for radiationless conversion, and k_t is the rate constant for triplet formation. The steady-state distribution between the excited species is determined by the rate constants $k_a[A]$ and k_d, but the rate of formation of each of these is given by R_M and R_D. The mechanism given in (7) is completely general for any luminescent process, even ecl. Its subsequent application, though, is based upon the assumption that steady-state luminescence is achieved. Prior to rrde ecl, this was not possible, however. The steady-state treatment is simplified by defining τ_D and τ_M, and the lifetimes of the excimer and monomer respectively, as

$$1/\tau_D = k_f' + k_0' + k_d \qquad (8)$$

(13) C. A. Parker and C. G. Hatchard, *Trans. Faraday Soc.*, **59**, 284 (1963).
(14) C. A. Parker and G. D. Short, *ibid.*, **63**, 2618 (1967).
(15) J. B. Birks, *J. Phys. Chem.*, **67**, 1299 (1963).

and

$$1/\tau_M = k_f + k_0 + k_t \qquad (9)$$

The steady-state equations for the general mechanism then become

$$([1/\tau_M] + k_a[A])[A^*] = R_M + k_d[A_2^*] \qquad (10)$$

and

$$[A_2^*]/\tau_D = R_D + k_a[A][A^*] \qquad (11)$$

Therefore, the ratio ϕ_D/ϕ_M, the relative excimer emission, is given by

$$\frac{\Phi_D}{\Phi_M} \equiv \frac{k_f'[A_2^*]}{k_f[A^*]} =$$

$$\frac{k_f'}{k_f} \frac{\tau_D}{1 + \alpha\tau_D k_d} \left(\frac{\alpha}{\tau_M} + (1 + \alpha)k_a[A] \right) \qquad (12)$$

where α is equal to R_D/R_M. For prompt fluorescence, R_D, and thus α, is zero, so that (12) reduces to

$$\Phi_D/\Phi_M = \frac{k_f'}{k_f}\tau_D k_a[A] = m_1[A] \qquad (13)$$

This is an equation of a straight line passing through the origin, so that in prompt fluorescence the relative excimer emission is directly proportional to the bulk concentration of the hydrocarbon. On the other hand, if some process such as that in (6) contributes to the direct formation of the excimer, neither R_D nor α is zero. In this event, the relative excimer emission is still linear with hydrocarbon concentration, but (12) now gives an intercept of $(k_f'/k_f)(\tau_D/\tau_M)[\alpha/(1 + \alpha\tau_D k_d)]$ and a slope of $[(1 + \alpha)/(1 + \alpha\tau_D k_d)](k_f'/k_f)\tau_D k_a$, which can be no less than m_1 of (13). Therefore, if these characteristics are observed, some process such as triplet–triplet annihilation contributes to the direct formation of the excimer.

The observation that the ecl spectrum of pyrene in Figure 14 exhibits a higher relative excimer emission than the fluorescence spectrum shown in the same figure indicates that some process may contribute to the direct formation of the excimer in energy-deficient pyrene ecl. Hence, the validity of (13) was tested by measuring the relative excimer emission Φ_D/Φ_M at several different pyrene concentrations for both prompt fluorescence and ecl. In all cases Φ_D/Φ_M was determined by cut-and-weigh integrations of these two portions of the spectrum. No TMPD was present in the DMF solutions of pyrene used in the fluorescence experiments, but the ecl determinations had to be carried out in the presence of 1.0 mM TMPD. Experiments described below demonstrate that Φ_D/Φ_M is relatively insensitive to TMPD concentration at low concentrations. The results of these measurements are shown in Figure 17. In this figure, line a shows the variation of relative excimer emission in ecl as a function of bulk pyrene concentration. The spectra which were integrated to obtain these points were obtained by generating a constant current (about 35 μA) of $TMPD\cdot^+$ at the disk while maintaining the ring at potentials which would generate $P\cdot^-$; different solutions were used for each trial. Line b shows the same ratio for prompt fluorescence. Both these lines demonstrate effects predicted by (13). Most important, a definite intercept is observed for line a, indicating that some process con-
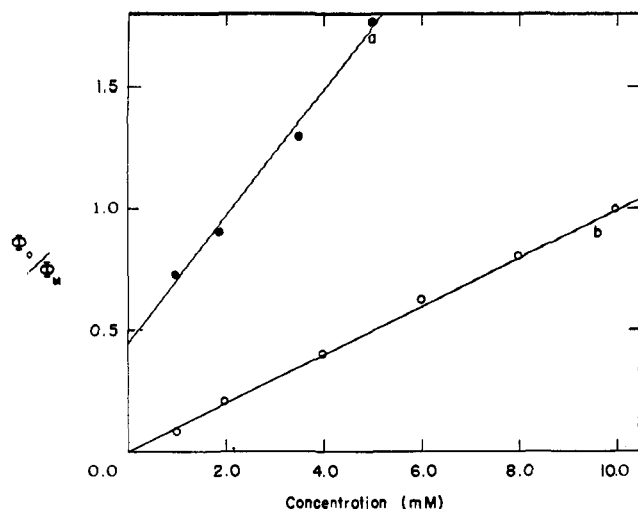
Figure 17. Relative pyrene excimer emission as a function of pyrene concentration in (a) ecl and (b) fluorescence.

Figure 18. Ecl efficiency for the pyrene–TMPD system as a function of TMPD concentration.

tributes to the direct formation of the excimer so that in ecl R_D and α are not zero. In view of the energy-deficient nature of the initial reaction of TMPD·+ and P·⁻ and the obvious necessity of a second elementary reaction to produce P_2*, the triplet–triplet annihilation scheme, (6), is a most appealing way of achieving the required direct population of the excimer.

Effects of TMPD Quenching. Several of the ecl experiments could be explained by TMPD quenching of pyrene fluorescence and pyrene ecl. In the spectra shown in Figure 14, the addition of TMPD has the obvious effect of decreasing the relative excimer emission. The low efficiency measurements shown in Table II may also be attributed to TMPD quenching. After some preliminary fluorescence experiments indicated that the addition of TMPD to a DMF solution of pyrene lowered the pyrene fluorescence, it was decided to investigate the TMPD quenching of pyrene in more detail.

The effect of TMPD quenching on pyrene ecl was studied by the techniques employed in the quenching experiments performed on DPA ecl. The special cell equipped with the high-pressure bulb was used to vary the TMPD concentration while holding the pyrene concentration constant and keeping the cell in a fixed position. Constant pyrene concentration was maintained by preparing both the solution in the cell and the solution in the bulb from the same stock DMF solution that was 3.5 mM in pyrene and 0.1 M in TBAP; the concentration of TMPD was determined by cyclic voltammetry. The efficiency of the reaction of TMPD·+ and P·⁻ was determined by generating a constant current of TMPD·+ at the disk while producing P·⁻ at the ring; since each measurement required a complete spectrum to determine the absolute intensity of the ecl emission, only two spectra were obtained at each concentration of TMPD. The dependence of ecl efficiency upon TMPD concentration is shown in Figure 18. The initial apparent efficiency in this figure is somewhat higher than those reported in Table II; this is probably because a different cell was used and the bulk concentration of pyrene was lower in this determination. Many of the remarks made concerning TMPD quenching of DPA ecl also apply in this case. Clearly, the effect of increasing the TMPD concentra-
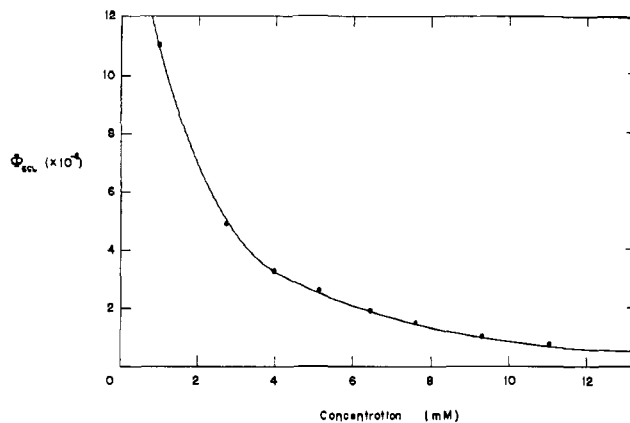
tion is to decrease the efficiency of the ecl reaction, and just as in the parallel DPA studies, the effect can only be attributed to TMPD. Unlike the DPA studies, however, no reasonable estimate of the half-quenching concentration may be made because no concentration of TMPD used was so small as to be ineffective in quenching emission. Since the same concentration range was used in both studies, this indicates that TMPD is far more effective at quenching energy deficient pyrene ecl.

It is of interest to note that even though the total ecl emission is decreased by TMPD, the relative excimer emission in ecl is only changed at large (about 10 mM) concentrations of TMPD. This means that the data given in Figure 17a do not depend upon TMPD concentration. As shown in Figure 14, however, the relative excimer emission in fluorescence is much more dependent upon TMPD concentration.

These general observations about TMPD quenching prompted an extension of the treatment given by Parker and coworkers and Birks to include the effect of bimolecular quenching on the mechanism given by (7). Specifically, this involved the addition of the quenching reactions

$$A^* + Q \xrightarrow{k_1} A + Q \qquad (14)$$

$$A_2^* + Q \xrightarrow{k_2} 2A + Q \qquad (15)$$
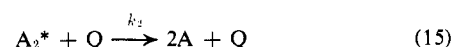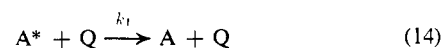
where Q represents the added quencher (*i.e.*, TMPD), to the general mechanism scheme. This is accomplished most readily by including the quenching rates $k_1[Q]$ and $k_2[Q]$ in the lifetimes of the monomer and the excimer so that

$$1/\tau_M' = k_f + k_0 + k_t + k_1[Q] = (1/\tau_M) + k_1[Q] \quad (16)$$

and

$$1/\tau_D' = k_f' + k_0' + k_d + k_2[Q] =$$
$$(1/\tau_D) + k_2[Q] \quad (17)$$

By treating the problem in this way, the algebraic operations required to include the effect of bimolecular quenching are no different from those used in the original derivation, so one need only replace τ_D and τ_M in (12) with τ_D' and τ_M' to obtain a solution

$$\frac{\Phi_D}{\Phi_M} = \frac{k_f'}{k_f} \frac{\tau_D'}{1 + \alpha\tau_D'k_d}\left(\frac{\alpha}{\tau_M'} + (1 + \alpha)k_a[A]\right) \quad (18)$$
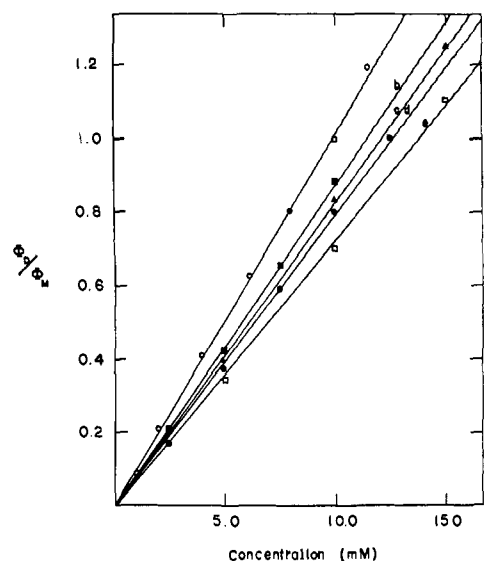
Figure 19. Relative pyrene excimer emission from fluorescence studies in the presence of TMPD. Each line shows the variation of Φ_D/Φ_M with pyrene concentration at TMPD concentrations of (a) 0, (b) 0.3, (c) 0.5, (d) 0.6, and (e) 1.0 mM.

Figure 20. Reciprocal slope of lines in Figure 19 as a function of TMPD concentration.

When some process contributes to the direct formation of the excimer and α does not equal zero, this solution is sufficiently complex to accommodate the observation that in ecl the relative excimer emission is somewhat insensitive to changes in [Q]; increasing [Q] lowers both τ_D' and τ_M', and when α is nonzero, these have an opposite effect on Φ_D/Φ_M.

On the other hand, in prompt fluorescence when α is zero, the effect of τ_M' is eliminated and a result similar to that of (13) is obtained so that

$$m_1 = (k_f'/k_f)\tau_D'k_a \tag{19}$$

The relative excimer emission is still predicted to be linear with [A]; the slope of the line will decrease with increasing [Q] because τ_D' decreases with increasing [Q].

The combination of (17) and (19) yields the result

$$m_1^{-1} = (k_f/k_f'k_a)([1/\tau_D] + k_2[Q]) \tag{20}$$

This states that m_1^{-1}, the reciprocal slope of the Φ_D/Φ_M vs. [A] plot, is a linear function of [Q], with slope $k_2k_f/k_f'k_a$ and intercept $k_f/k_f'k_a\tau_D$. Therefore, the ratio of the slope to the intercept in the m_1^{-1} vs. [Q] plot is $k_2\tau_D$.

The fluorescence quenching experiments suggested by (20) were performed to study the effect of TMPD quenching of the pyrene excimer. The initial results of this study are shown in Figure 19, where Φ_D/Φ_M is plotted as a function of pyrene concentration in DMF solution. The upper line is identical with that shown in Figure 17b; it was obtained in the absence of TMPD. Each line clockwise from it in Figure 19 was obtained in the presence of a successively higher concentration of TMPD so that the slope decreases with increasing TMPD concentration, as predicted by (19).

When the reciprocal slope of Figure 19 is plotted as a function of the TMPD concentration used in each experiment, the straight-line behavior of Figure 20 is
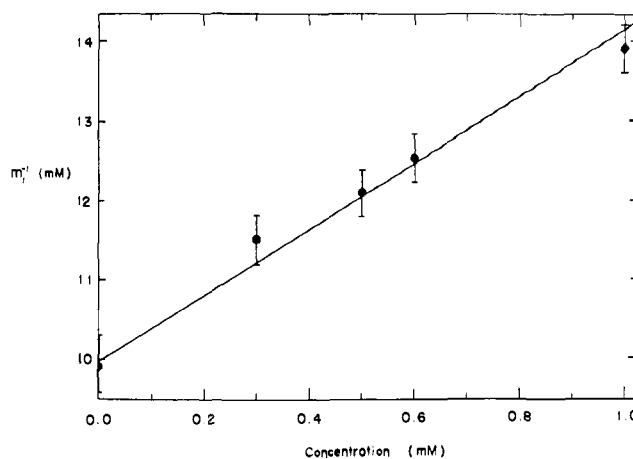
obtained. As demonstrated above, the slope of Figure 20 divided by its intercept will yield $k_2\tau_D$, and when this is done, a value of $k_2\tau_D = 0.4$ m$M^{-1} = 4 \times 10^2$ M^{-1} is obtained.

The lifetime of the pyrene dimer has been reported by Birks and Munro[16] to be 4×10^{-8} sec in ethanol solution. If one accepts this as a valid estimate of the lifetime of the excimer in DMF, the bimolecular quenching rate constant k_2 is about 10^{10} M^{-1} sec^{-1}. This is very close to the diffusion-controlled rate constant in DMF solutions. Thus, it is reasonable to believe that pyrene excimer quenching by TMPD proceeds at diffusion-controlled rates.

This result is very useful in explaining the low efficiencies obtained in pyrene ecl, because pyrene is the only compound studied which has an excimeric form with a lifetime long enough to fluoresce. This added longevity of the pyrene excimer subjects it to the added probability of diffusion-controlled TMPD attack. Thus, it is likely that this extra mode of rapid quenching accounts for the low efficiencies observed above.

Conclusions

The utility of the rrde in ecl studies has been demonstrated. The low efficiency of ecl clearly suggests that consideration of quenching by radical ions and parent materials is important in a complete description of the ecl process. Potential-scan experiments have shown that excited-state intermediates can be produced by reaction of anion radicals with dications as well as cation radicals, in support of previous work which demonstrated that a variety of oxidants can be employed with anion radicals to produce ecl. The low efficiencies of energy-deficient systems and the quenching experiments with the pyrene–TMPD system lend further support to the existence of triplet intermediates and the triplet–triplet annihilation mechanism for these cases.

(16) J. B. Birks and I. H. Munro in "Luminescence in Organic and Inorganic Materials," H. P. Kallmann and G M. Spruch, Ed., Wiley, New York, N. Y., 1962.